

Three mode Er³⁺ ring-doped fiber amplifier for mode-division multiplexed transmission

Y. Jung,^{1,*} Q. Kang,¹ V. A. J. M. Sleiffer,² B. Inan,³ M. Kuschnerov,⁴ V. Veljanovski,⁴ B. Corbett,⁵ R. Winfield,⁵ Z. Li,¹ P. S. Teh,¹ A. Dhar,¹ J. Sahu,¹ F. Poletti,¹ S. -U. Alam,¹ and D. J. Richardson¹

¹Optoelectronics Research Centre, University of Southampton, Southampton, SO17 1BJ, UK

²COBRA institute, Eindhoven University of Technology, The Netherlands

³Institute of Communications Engineering, Technische Universität München, Munich, Germany

⁴Nokia Siemens Networks GmbH & Co. KG, Munich, Germany

⁵Tyndall National Institute, Cork, Ireland

*ymj@orc.soton.ac.uk

Abstract: We successfully fabricate three-mode erbium doped fiber with a confined Er³⁺ doped ring structure and experimentally characterize the amplifier performance with a view to mode-division multiplexed (MDM) transmission. The differential modal gain was effectively mitigated by controlling the relative thickness of the ring-doped layer in the active fiber and pump launch conditions. A detailed study of the modal gain properties, amplifier performance in a MDM transmission system and inter-modal cross-gain modulation and associated transient effects is presented.

©2013 Optical Society of America

OCIS codes: (060.0060) Fiber optics and optical communications; (060.2320) Fiber optics amplifiers and oscillators.

References and links

1. A. D. Ellis, J. Zhao, and D. Cotter, "Approaching the non-linear Shannon limit," *J. Lightwave Technol.* **28**(4), 423–433 (2010).
2. R.-J. Essiambre, G. Kramer, P. J. Winzer, G. J. Foschini, and B. Goebel, "Capacity limits of optical fiber networks," *J. Lightwave Technol.* **28**(4), 662–701 (2010).
3. P. J. Winzer and G. J. Foschini, "MIMO capacities and outage probabilities in spatially multiplexed optical transport systems," *Opt. Express* **19**(17), 16680–16696 (2011).
4. R. Ryf, S. Randel, A. H. Gnauck, C. Bolle, A. Sierra, S. Mumtaz, M. Esmaelpour, E. C. Burrows, R. Essiambre, P. J. Winzer, D. W. Peckham, A. H. McCurdy, and R. Lingle, "Mode-division multiplexing over 96km of few-mode fiber using coherent 6x6 MIMO processing," *J. Lightwave Technol.* **30**(4), 521–531 (2012).
5. S. Randel, R. Ryf, A. Sierra, P. J. Winzer, A. H. Gnauck, C. A. Bolle, R. J. Essiambre, D. W. Peckham, A. McCurdy, and R. Lingle, Jr., "6x6-MIMO mode-division multiplexed transmission over 33-km few-mode fiber enabled by 6x6 MIMO equalization," *Opt. Express* **19**(17), 16697–16707 (2011).
6. N. Bai, E. Ip, Y. K. Huang, E. Mateo, F. Yaman, M. J. Li, S. Bickham, S. Ten, J. Liñares, C. Montero, V. Moreno, X. Prieto, V. Tse, K. Man Chung, A. P. T. Lau, H. Y. Tam, C. Lu, Y. Luo, G. D. Peng, G. Li, and T. Wang, "Mode-division multiplexed transmission with inline few-mode fiber amplifier," *Opt. Express* **20**(3), 2668–2680 (2012).
7. C. Koebele, M. Salsi, D. Sperti, P. Tran, P. Brindel, H. Mardoyan, S. Bigo, A. Boutin, F. Verluise, P. Sillard, M. Astruc, L. Provost, F. Cerou, and G. Charlet, "Two mode transmission at 2x100 Gb/s, over 40 km-long prototype few-mode fiber, using LCOS-based programmable mode multiplexer and demultiplexer," *Opt. Express* **19**(17), 16593–16600 (2011).
8. Y. Jung, S. Alam, Z. Li, A. Dhar, D. Giles, I. P. Giles, J. K. Sahu, F. Poletti, L. Grüner-Nielsen, and D. J. Richardson, "First demonstration and detailed characterization of a multimode amplifier for space division multiplexed transmission systems," *Opt. Express* **19**(26), B952–B957 (2011).
9. Y. Jung, S. Alam, Z. Li, A. Dhar, D. Giles, I. Giles, J. Sahu, L. Grüner-Nielsen, F. Poletti, and D. Richardson, "First demonstration of multimode amplifier for spatial division multiplexed transmission systems," in *37th European Conference and Exposition on Optical Communications, OSA Technical Digest (CD)* (Optical Society of America, 2011), paper Th.13.K.4.
10. Q. Kang, E. L. Lim, Y. Jung, J. K. Sahu, F. Poletti, C. Baskiotis, S. U. Alam, and D. J. Richardson, "Accurate modal gain control in a multimode erbium doped fiber amplifier incorporating ring doping and a simple LP01 pump configuration," *Opt. Express* **20**(19), 20835–20843 (2012).
11. V. A. J. M. Sleiffer, Y. Jung, V. Veljanovski, R. G. H. van Uden, M. Kuschnerov, Q. Kang, L. Grüner-Nielsen, Y. Sun, D. J. Richardson, S. Alam, F. Poletti, J. K. Sahu, A. Dhar, H. Chen, B. Inan, A. M. J. Koonen, B. Corbett, R. Winfield, A. D. Ellis, and H. de Waardt, "73.6Tb/s (96x3x256-Gb/s) mode-division-multiplexed DP-

- 16QAM transmission with inline MM-EDFA,” in *38th European Conference and Exposition on Optical Communications*, OSA Technical Digest (CD) (Optical Society of America, 2012), paper Th.3.C.
12. V. A. J. M. Sleiffer, Y. Jung, V. Veljanovski, R. G. H. van Uden, M. Kuschnerov, H. Chen, B. Inan, L. G. Nielsen, Y. Sun, D. J. Richardson, S. U. Alam, F. Poletti, J. K. Sahu, A. Dhar, A. M. J. Koonen, B. Corbett, R. Winfield, A. D. Ellis, and H. de Waardt, “73.7 Tb/s (96 x 3 x 256-Gb/s) mode-division-multiplexed DP-16QAM transmission with inline MM-EDFA,” *Opt. Express* **20**(26), B428–B438 (2012).
 13. C. R. Giles, E. Desurvire, and J. R. Simpson, “Transient gain and cross talk in erbium-doped fiber amplifiers,” *Opt. Lett.* **14**(16), 880–882 (1989).
 14. Y. Sun, J. L. Zyskind, A. K. Srivastava, and L. Zhang, “Analytical formula for the transient response of erbium-doped fiber amplifiers,” *Appl. Opt.* **38**(9), 1682–1685 (1999).
 15. A. K. Srivastava, Y. Sun, J. L. Zyskind, and J. W. Sulhoff, “EDFA transient response to channel loss in WDM transmission system,” *IEEE Photon. Technol. Lett.* **9**(3), 386–388 (1997).
 16. P. C. Becker, N. A. Olsson, and J. R. Simpson, *Erbium-Doped Fiber Amplifiers: Fundamentals and Technology* (Academic Press, 1999), Chap. 2.
 17. J. E. Townsend, S. B. Poole, and D. N. Payne, “Solution-doping technique for fabrication of rare-earth-doped optical fibres,” *Electron. Lett.* **23**(7), 329–331 (1987).
 18. K. Lyytikäinen, S. Huntington, A. Carter, P. McNamara, S. Fleming, J. Abramczyk, I. Kaplin, and G. Schötz, “Dopant diffusion during optical fibre drawing,” *Opt. Express* **12**(6), 972–977 (2004).
 19. F. Z. Tang, P. McNamara, G. W. Barton, and S. P. Ringer, “Multiple solution-doping in optical fibre fabrication II- Rare earth and aluminium co-doping,” *J. Non-Cryst. Solids* **354**(15-16), 1582–1590 (2008).
 20. N. Shukunami and S. Inagaki, “Doped optical fiber having core and clad structure for increasing the amplification band of an optical amplifier using the optical fiber,” US Patent 5,778,129 (1998).

1. Introduction

To date single mode fibers (SMFs) have been used as the transmission medium of choice in long-haul telecommunication systems, with the use of multimode fibers (MMFs) restricted to short distance (e.g. local area) networks due to their severe inter-modal dispersion which grossly limits the transmission bandwidth. However, driven by fears of a future “capacity crunch” [1–3], major interest is developing in the potential use of Mode Division Multiplexing (MDM) in which selective mode excitation and detection schemes are used to define distinguishable information channels within a few mode fiber (FMF) [4–7]. Since the modes are orthogonal, it is in principle possible to increase the capacity in accordance with the number of modes supported by the FMF. Digital signal processing can be utilized to mitigate transmission impairments caused by mode-coupling in MDM systems and thereby to substantially increase the achievable transmission distance. However, in order to be useful in long-haul systems, a practical high-performance FMF amplifier is essential. In our recent work [8, 9], we successfully demonstrated a multimode (three-mode) erbium-doped fiber amplifier (TM-EDFA) for MDM applications providing simultaneous modal gains of ~20dB for different pair-wise combinations of spatial and polarization modes. We achieved a relatively low differential mode gain (DMG) of <3dB through the use of pump mode control and a special erbium doped fiber (EDF) design incorporating increased doping (both index-modifying and erbium) at the edges of the core. Whilst good performance was achieved significant scope exists for new fiber designs providing simplified means of DMG control and improved overall gain performance. To address this we have recently theoretically proposed a two-mode group (i.e. three distinct modes LP_{01} , LP_{11a} , LP_{11b}) EDF design incorporating localized ring doping where the erbium ions are confined in a ring within the fiber core [10].

In this paper, we have experimentally evaluated the feasibility of using ring-doping to provide simplified means of DMG control and obtained improved overall gain performance. Section 2 details an investigation of the modal gain properties and the amplifier performance of the ring-doped TM-EDFA. In order to reliably use this device in full data transmission experiments a far more detailed understanding of how the amplifier performs under fully-loaded conditions (both in terms of DWDM channels across the C-band and the full set of supported modes) is required. Section 3 details the impact of the input signal power and pump power levels on the spectral gain flatness and bit error rate (BER) performance of the fully-loaded amplifier. The optimum conditions required to obtain low power penalty operation are also discussed. Note that following characterization of the TM-EDFA the device was successfully used in the 96-channel, 73.7 Tbit/s MDM transmission experiments reported in our recent publications [11, 12]. One of the most interesting, but to date uninvestigated,

aspects of MM-EDFA operation, is the impact of cross-gain modulation and the associated gain dynamics (e.g. the transient response) both between (and indeed within) spatial mode groups as the number of channels within the device is changed. Such effects, already extensively studied both theoretically and experimentally for single mode EDFAs [13–15], represents an important issue in enabling practical application of MDM technology within robustly reconfigurable optical networks. A detailed investigation of the power excursions due to cross gain modulation and the corresponding transient times of a TM-EDFA supporting two LP mode groups (LP_{01} and LP_{11}) are discussed in Section 4.

2. Modal gain performance in a ring-doped TM-EDF

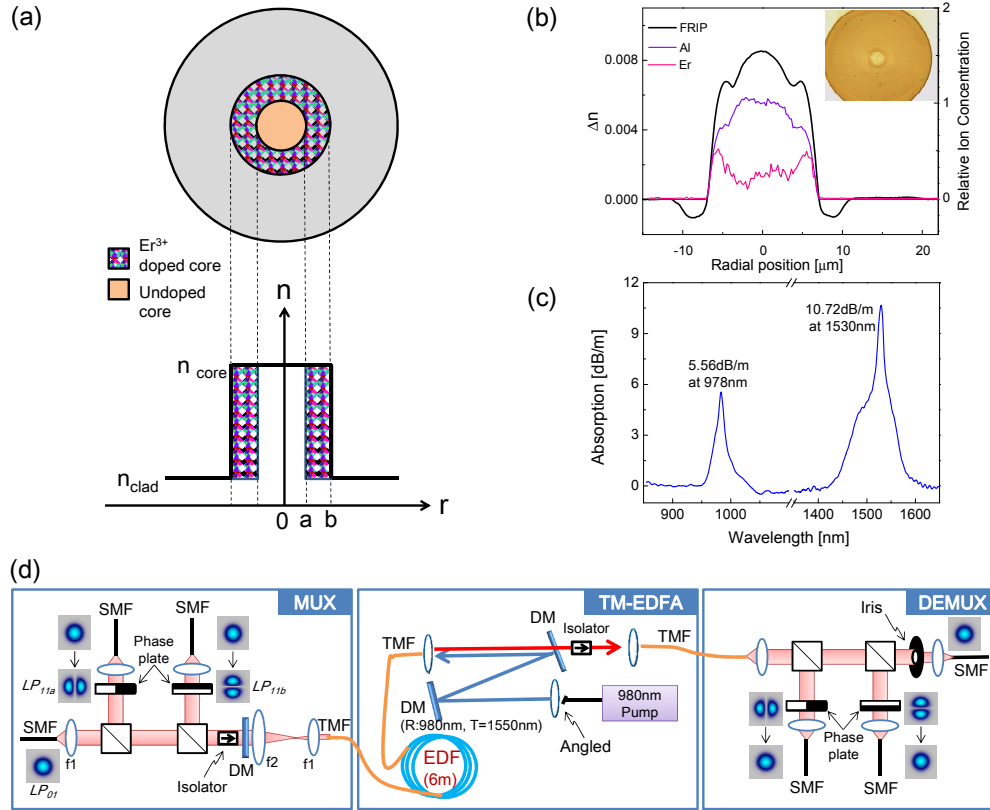


Fig. 1. Three mode Er^{3+} ring-doped fiber: (a) schematic design, (b) fiber refractive index/doping profile, and (c) measured absorption spectrum. (d) The measurement setup for modal gain analysis of the amplifier: mode multiplexer (MUX), three mode erbium doped fiber amplifier (TM-EDFA) and mode demultiplexer (DEMUX).

The multimode erbium ring-doped fiber has a two layer core structure with different doping compositions between layers as shown schematically in Fig. 1(a). The outer core region is designed to be doped with active Er^{3+} ions with Al_2O_3 as a co-dopant, whilst the inner core is doped only with Al_2O_3 with a concentration designed to ensure that the refractive indices of the two regions are well matched. The ring-doped TM-EDF was fabricated using the well-established modified chemical vapor deposition (MCVD) process coupled with solution doping [16, 17]. First, a porous SiO_2 core layer was deposited inside a silica tube and immersed in a methanol solution containing salts of erbium and aluminum co-dopants and then sintered into glass to obtain the erbium doped region. Secondly, a pure Al_2O_3 silica layer (without Er^{3+} ions) was further deposited to produce a central index-matched step index core. A normalized ring thickness (a/b) of 0.48 was targeted in the first instance in accordance with

the estimated optimum value for DMG minimization for the step index fiber from reference [10]. The resultant refractive index profile of the fiber preform deviates slightly from that of an ideal step index profile and a small refractive index discontinuity between the inner and outer core was observed as illustrated in Fig. 1(b). We believe that the sintering process after the solution doping induces a loss of erbium and aluminum oxides from the core causing a slight index dip in the proximity of the interface between inner and outer core regions. The dopant distribution in the fiber preform was measured by secondary ion mass spectroscopy (SIMS) which showed that the refractive index profile closely follows the radial distribution of aluminum. Note however that although the erbium dopants are clearly concentrated within a distinct ring in the outer core region, undesired diffusion of Er^{3+} towards the center of the core is seen to have occurred. Diffusion of erbium ions is to be expected to some degree during the final tube collapse and/or additionally during the fiber drawing process, with the extent dependent on several factors including the composition of the glass host, the detailed nature of the heat treatment during collapse, the duration of the collapse process, and the fiber drawing temperature itself [18–20]. It may be possible to reduce this lateral dopant diffusion in future fibers by depositing a thin layer of pure SiO_2 as a diffusion barrier between the inner and outer core regions [20]. The experimental preform parameters were then fed back into the numerical modeling tool described in [10] to ascertain the required final fiber core diameter for low DGD. Based on the results of these numerical simulations, a fiber was drawn with an outer cladding diameter of $111\mu\text{m}$, an inner core diameter of $7.7\mu\text{m}$ and a corresponding erbium-doped ring thickness of $2.6\mu\text{m}$. The estimated effective NA of the core is ~ 0.14 . The measured absorption at 980nm is 5.56dB/m (as shown in Fig. 1(c)), and the background loss is 21.4dB/km at 1285nm .

To measure the modal gain properties of the ring-doped TM-EDFA, we constructed a mode multiplexer, multimode amplifier and demultiplexer as shown in Fig. 1(d). In the mode multiplexer, three spatial modes (LP_{01} , LP_{11a} , LP_{11b}) were multiplexed using free space optics and polymethyl methacrylate (PMMA) phase plates were used to selectively excite the LP_{11} modes from an incident LP_{01} beam. All three spatial modes were combined using two beam splitters and coupled into a short length ($\sim 10\text{m}$) of passive three mode fiber (TMF). To provide clean mode-excitation, a telecentric lens system ($f_1 = 3.1\text{mm}$, $f_2 = 125\text{mm}$) was used and an extinction ratio of $> 25\text{dB}$ was achieved. A dichroic mirror (high reflection @ 980nm and high transmission @ 1550nm) was used to reject any unabsorbed pump power while a polarization-insensitive isolator was used to suppress any signal light propagation in the backward direction. The passive TMF was then spliced directly to the ring-doped active fiber and a 980nm pump laser was free-space coupled into the TM-EDF following reflection from two dichroic mirrors. The amplified output was coupled into another 10m -length of TMF and was demultiplexed into three spatial channels using our mode DEMUX.

First of all, for simple but effective modal gain measurement, different wavelengths were chosen for the seed signals for two different channels (1550nm for the LP_{01} and 1555nm for the LP_{11}) and the combination of a tunable narrow bandpass filter ($\Delta\lambda = 2\text{nm}$) and a power meter were used at the output of the amplifier to separate the individual channels, similar to the setup described in Ref [8]. Figure 2(a) shows the mode dependent gain for central pump launch conditions measured as a function of the launched pump power for several different lengths of ring-doped EDF. The input signal power per channel was fixed at -2.5dBm . For a 2m length of EDF, the maximum achievable modal gain was 10.7dB for the LP_{01} mode and 9.9dB for the LP_{11} mode, respectively. At a fixed pump power of 21dBm , the gain for the LP_{01}

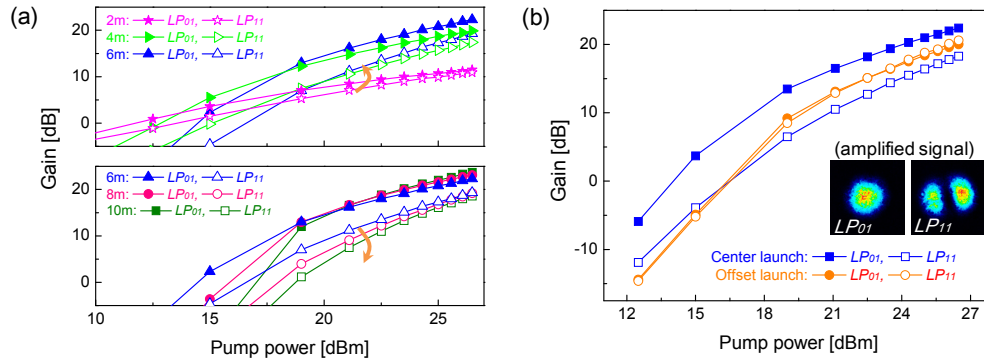


Fig. 2. (a) The effect of the length of ring-doped TM-EDFA on the modal gain and (b) the effect of pump launch condition on modal gain as a function of pump power at an input signal power of -2.5 dBm per mode

mode increased monotonically from 8.5 dB to 16.6 dB as the length of EDF was increased from 2 m to 10 m. However, the gain of the LP_{11} mode increased from 7.1 dB to 11.2 dB for a 6 m-length of fiber and then begins to decrease to 7.5 dB for further increases in EDF length. This behavior is due to the fact that with a counter-propagating central pump launch in conjunction with longer EDF lengths the LP_{11} mode ordinarily experiences greater absorption under normal pumping conditions than the LP_{01} mode at the signal input end where the population inversion is lowest (due to the greater spatial overlap with the dopant). Moreover, this choice of pump excitation ensures that the LP_{01} mode sees the population inversion earlier than the LP_{11} mode, resulting in a faster growth of the power of the LP_{01} mode. For a pump power of 21 dBm, the optimum EDF length was found to be 6 m and the differential modal gain was measured to be ~ 5 dB as shown in Fig. 2(b). This mode dependent gain can be eliminated by using an offset pump launch (which excites a combination of symmetric and asymmetric modes) at a pump power of around 22–23 dBm. For higher pump powers with the same offset launch condition, the gain for the LP_{11} mode tends to become higher than that for the LP_{01} mode. Although these results demonstrate that the differential mode gain can be effectively mitigated using the fabricated ring-doped EDF in conjunction with offset pump launch condition we ultimately expect that it will be possible to achieve zero mode dependent gain for the simpler and more convenient case of a central pump launch by producing fiber with a better defined annular dopant distribution [10].

2. System performance of a ring-doped TM-EDFA

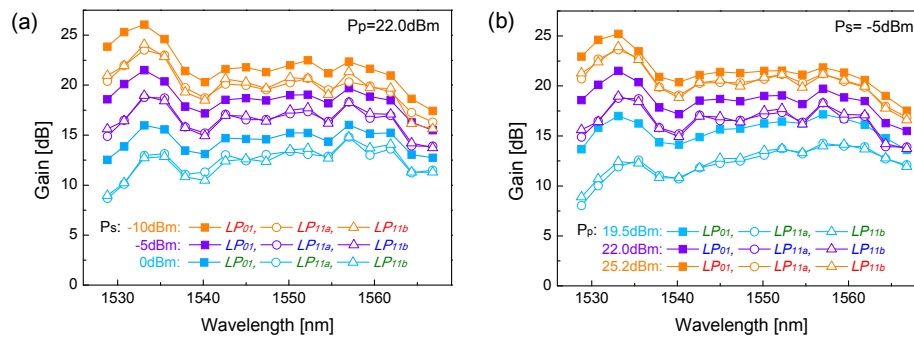


Fig. 3. Measured gain spectrum characteristics for (a) different input signal powers (P_s) and (b) pump powers (P_p).

To evaluate the performance of the ring-doped TM-EDFA in a transmission system, 17 external cavity lasers at distinct wavelengths across the C-band were multiplexed and modulated with 256-Gb/s DP-16QAM using an IQ-modulator and polarization-multiplexing stage. The data stream was split up into three equally powered signals and fed to the mode multiplexer (MUX) as described in [2]. A 6m long ring-doped TM-EDF was used as the gain medium in conjunction with offset pump launch to reduce the mode dependent gain.

2.1 Gain spectra and BER performance of the TM-EDFA

First, the gain spectrum of the TM-EDFA was investigated for different (launched) input signal powers per spatial mode (including both polarizations and all 17 channels) as shown in Fig. 3. An offset pump launch condition was applied to maximize the gain for the LP_{11} modes and the total launched pump power was fixed at 22dBm. For an input signal power of -10 dBm per mode, the average gain across the full C-band was 22dB for the LP_{01} and 20dB for the LP_{11} modes. Both modes experience gain reduction with an increase in input signal power and the gain flatness improves as the EDFA becomes more deeply saturated. Figure 3(b) shows the gain spectra of the amplifier for different pump powers at a fixed input signal power of -5 dBm per mode. As the pump power increases from 19.5dBm to 25.2dBm, both the modal gains were increased and the differential modal gain was improved from ~ 5 dB to ~ 1 dB. Note also that the gain peak shifts from 1560nm to 1530nm.

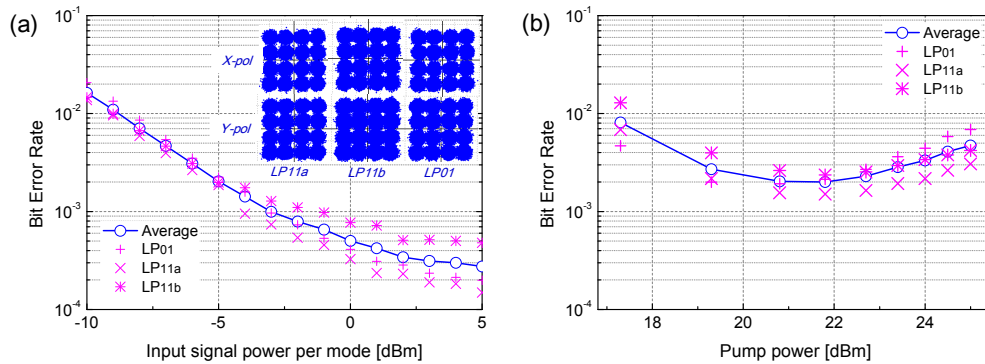


Fig. 4. BER performance of the TM-EDFA as a function of (a) input signal power per mode and (b) launched pump power. The constellations are the recovered 256-Gb/s DP-16QAM at an input signal power of -5 dBm per mode.

To evaluate the bit error rate (BER) performance, the three output ports of the DEMUX were plugged into 50GHz tunable optical filters and commercial coherent receivers. The samples obtained from the digital sampling scopes were recorded and processed offline using data-aided digital signal processing. Figure 4(a) shows the BER measurement results for the TM-EDFA as a function of the input signal power per mode at a fixed pump power of 22dBm. It is clearly seen that the BER performance is highly dependent on the input signal power and that too low an input signal power leads to a rapid degradation in the BER, due to the increased level of ASE (reduced optical signal to noise ratio (OSNR)). We also tested the BER performance of the amplifier for various pump powers at a fixed input signal power of -5 dBm per mode. As depicted in Fig. 4(b), the experimental BER curve shows that an optimum pump power exists that gives the best BER performance for a given input signal power. Generally, the higher the population inversion, the lower the amplifier noise figure. Thus, at low pump powers (<22 dBm), the BER was improved with an increase in pump power due to the increased population inversion towards the input end of the amplifier preventing absorption of the input signal and resulting in OSNR improvement. However as the pump power was increased even further (>22 dBm), the population inversion at the output end of the amplifier (which was also the pumping end) became significantly higher than that

required for the amplification of the incoming signal. The excess population inversion contributed to the generation of ASE within the TM-EDFA resulting in a drop in OSNR and the degradation in BER.

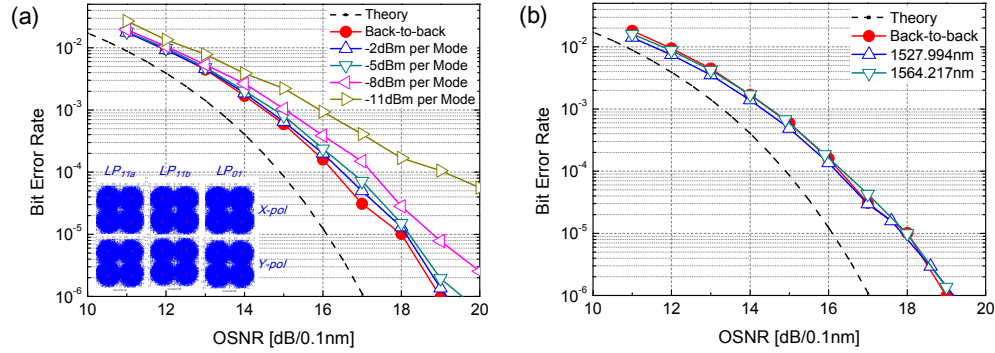


Fig. 5. (a) The measured BER performances at 1550.2 nm for various input signal power into the TM-EDFA and (b) measured BER at the edge channels of C-band (1527.994nm and 1564.217nm) at the input signal power of -5dBm . The constellations are the recovered 112Gb/s DP-QPSK for an input signal power of -5dBm per mode with an OSNR of $15\text{dB}/0.1\text{nm}$.

Figure 5(a) shows the averaged BER curves of all spatial modes (LP_{01} , LP_{11a} and LP_{11b}) for a 112Gb/s DP-QPSK signal at the center wavelength of the C-band (1550.2nm). As described in Fig. 4(a), the overall BER performance is strongly dependent on the input signal power into the TM-EDFA and which effects the output OSNR. The induced power penalty from the TM-EDFA was 0.1, 0.2, 0.5 and 1.5dB , respectively, for the -2 , -5 , -8 and -11dBm input signal power per mode cases compared to the back-to-back condition (only MUX/DEMUX without amplifier). The observed power penalty is small but it could be further reduced by applying a gain flattening filter after the amplifier and reducing remnant Fresnel reflections from the fiber end facets. We further tested the BER performance of our MM-amplifier at the edge channels of the C-band (1527.994nm and 1564.217nm). As shown in Fig. 5(b), the edge channel also shows a good power penalty of less than 0.2dB at the input signal power of -5dBm per mode.

3. Gain dynamics within a TM EDFA

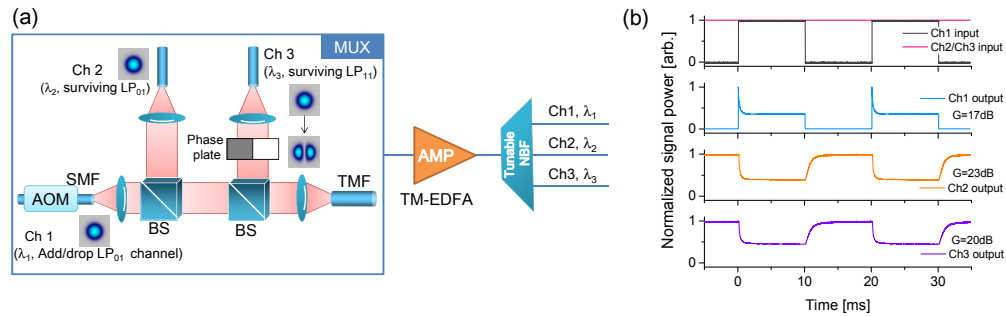


Fig. 6. (a) Experimental setup for investigating transient effects in a TM-EDFA. (b) Normalized input and output signal channels in the event of modulation of Ch1. BS: beam splitter, AOM: acousto-optic modulators, SMF: single mode fiber, TMF: three mode fiber, Ch1: channel 1, NBF: narrow bandwidth filter.

To investigate the gain dynamics within our ring-doped TM-EDFA, three channels at different wavelengths (two LP_{01} and one LP_{11}) were multiplexed using free space optics as shown in Fig. 6(a). An acousto-optic modulator (AOM) was placed in one of the LP_{01} lines, which we refer to as Ch1, and was used to generate a square wave with 50% duty cycle in order to allow us to simulate the impact of adding/dropping one (or multiple) spatial channels. Ch2 (LP_{01}) and Ch3 (LP_{11}) were used as “surviving channels” in order to investigate the mode dependent gain saturation and associated transient effects. The three mode fiber output from the multiplexer was spliced to a 6m-long length of ring-doped TM-EDFA and an offset pump launch scheme was adopted in order to minimize the gain differential between the LP_{01} and LP_{11} modes. For ease of demultiplexing the individual spatial channels at the output of the TM-EDFA, the wavelengths of Ch1, Ch2, and Ch3 were chosen to be 1548nm, 1553nm, and 1558nm respectively. A tunable narrow bandpass filter (NBF, $\Delta\lambda = 2\text{nm}$) was then used at the output of the amplifier to separate the individual spatial channels. The temporal response of each channel was recorded using 1.2GHz InGaAs photodiodes (DET01CFC, Thorlabs) and a digital oscilloscope (TDS5032B, Tektronix). Unless otherwise stated the input power for each channel was kept constant at -6dBm (which we take to be representative of the power of a single “data stream”) and the pump power was fixed at 23dBm .

3.1. Transient response of a TM-EDFA

Figure 6(b) shows the normalized input and output signal channels as one of the channels is modulated. The add/drop input channel Ch1 has a power of 1.78dBm (equivalent in average power terms to 6 data streams each of -6dBm power) and was modulated using the AOM with a 50% duty cycle at a frequency of 10 Hz. The input of the surviving channels was kept constant (Ch2 = -6dBm , Ch3 = -6dBm equivalent to the power of 1 data stream of -6dBm power). The temporal measurements of the output signal channels are shown in Fig. 6(b). All channels experience significant signal power excursions (defined as the ratio between the maximum and minimum channel power in the absence and presence respectively of the Ch1 signal) as a result of cross gain saturation in the TM-EDFA. During a “channel-add” event (presence of Ch1), the surviving channels experience a drop in output power due to the increased competition for gain from the available population inversion resulting from the presence of Ch1. Conversely, during a “channel-drop” event, the surviving channels experience a sudden increase in inversion due to the disappearance of Ch1 and the original output power levels are restored. It is to be noted that the transient responses of the two different spatial modes (LP_{01} in Ch2 and LP_{11} in Ch3) are very similar.

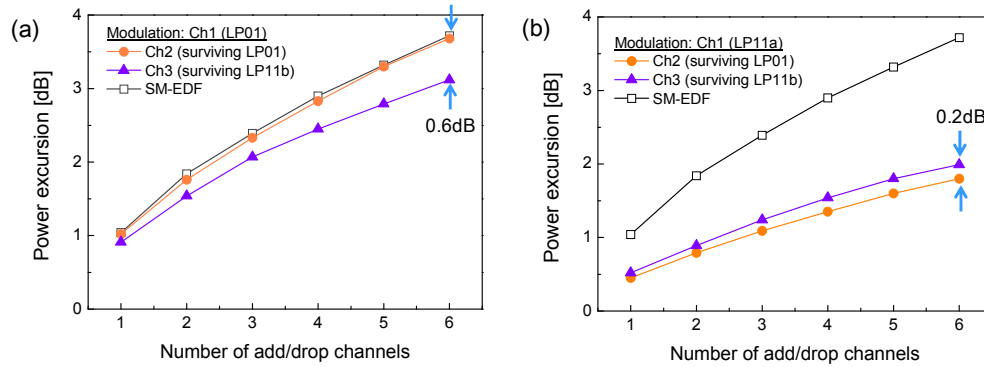


Fig. 7. Power excursion of surviving channels (LP_{01} and LP_{11}) according to Ch1 input signal power (equivalent to number of add/drop channels) in the event of either (a) LP_{01} or (b) LP_{11} spatial mode modulation.

To simulate the effects of adding/dropping multiple data streams the power of Ch1 (mode type: LP_{01}) was varied from -6dBm (1 data stream) to 1.78dBm (6 data streams). The results are shown in Fig. 7(a), where the power excursion for both Ch2 and Ch3 increases with Ch1 input signal power. For the surviving LP_{01} channel (Ch2), the power excursion increases from 1dB for the single data stream drop case to 3.7dB for the 6 stream case, whereas the increase is from 0.9dB to 3.1dB for the surviving LP_{11} channel (Ch3). The 0.6dB maximum power excursion difference between two spatial modes for a 6 data stream drop is due to the different spatial overlap between the LP_{01} and LP_{11} modes. Ch2 on the same LP_{01} spatial mode as modulated Ch1 sees a greater power excursion than Ch3 on the LP_{11} mode since it sees exactly the same spatial distribution of ions as Ch1. We would expect this difference to increase with an increasing number of add/drop data streams, or when operating the system more strongly in the large signal (saturated) regime. Note that the power excursion of the LP_{01} mode is very similar to that of the commercial single mode EDF tested (Fibercore I-25 used). To clearly check the modal dependence on gain dynamics, we altered the spatial mode type of the modulation port (Ch1) from LP_{01} to LP_{11} by inserting a binary phase plate. As shown in Fig. 7(b), for the LP_{11} modulation situation, the surviving LP_{11} (Ch2) shows a higher power excursion than the surviving LP_{01} channel (Ch3). The maximum power excursion difference was about 0.2dB.

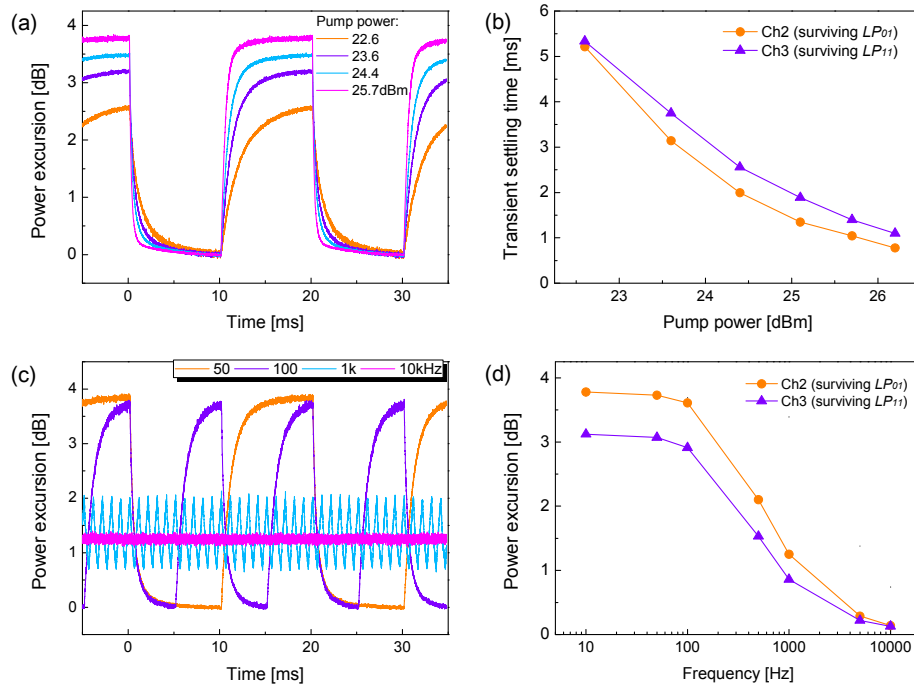


Fig. 8. The effect of pump power on gain dynamics as a function of (a) power excursion and (b) transient setting time. (c, d) Power excursion as a function of the modulation frequency.

To check the pump power dependence, we changed the pump power from 22.6dBm to 26.2dBm with a constant signal input power of Ch1 (1.78dBm). From Fig. 8(a), we can define the transient settling time (rise or fall time) as the time taken for the power excursion to go from 10% to 90% of the maximum steady state power excursion. In Fig. 8(b), we plot the measured transient settling time for both spatial modes. Both exhibit almost identical behavior with a settling time decreasing from 5.3ms to 1.1ms when increasing the pump power from 22.6dBm to 26.2dBm. Generally, the transient settling time is dependent on the level of saturation of the amplifier and in particular becomes shorter for higher pump or

signal powers. Consequently the transient response becomes faster as the pump power increases.

To examine the dependence of the power excursion on modulation frequency the modulation frequency of the AOM was gradually increased from 10Hz to 10kHz with a constant amplifier input signal power (Ch1 = 1.78dBm, Ch2 = -6dBm, Ch3 = -6dBm) and pump power (25.7dBm). As shown in Fig. 8(a), the total power excursion decreases as the modulation frequency is increased. At frequencies higher than 5kHz the surviving channels cannot follow the fast modulation and only a steady-state gain compression appears due to the slow response of the population inversion, which has an excited state lifetime of ~10ms. As shown in Fig. 8(d), the total power excursion for the LP_{01} and LP_{11} modes at 10Hz was 3.8dB and 3.2dB respectively, which decreased to less than 0.2dB at modulation frequencies higher than 5kHz.

4. Conclusion

We have experimentally investigated the performance of a multimode erbium ring-doped fiber, where the erbium ions are substantially confined within a ring within the fiber core, for a mode-division multiplexed system. The radial gain profiling with ring doping scheme led to significant differential modal gain mitigation. For an optimum offset pump launch condition, we observed that the differential modal gain becomes zero (virtually no mode dependent gain) at a moderate pump power and the gain of the LP_{11} mode tends to become higher than the LP_{01} mode for higher pump powers. Using the fabricated ring-doped TM-EDFA, we have quantified how the gain spectrum and BER performance were affected by input signal and pump power. Furthermore, we have investigated inter-modal cross gain and associated transient effects in a MM-EDFA for the first time. Our results indicate that all spatial modes experience roughly similar responses under a range of different add/drop conditions, but some evidence of mode dependent sensitivity was observed and the mode dependent gain dynamics was enhanced further when operating at higher levels of amplifier saturation.

Acknowledgment

This work was supported by the European Communities 7th Framework Programme under grant agreement 258033 (MODE-GAP).